Optimizing the Use of Groundwater Nitrogen (NO_3): Efficacy of the Pump and Fertilize Approach for Almond

Project No.: **15-PREC6-Smart**

Project Leader: David R. Smart
Viticulture and Enology
UC Davis
2142 Robert Mondavi Institute N
Davis, CA 95616
530.574.3929
drsmart@ucdavis.edu

Project Cooperators and Personnel:
Dr. Patrick Brown, Plant Sciences, UC Davis
Dr. Jan Hopmans, Dr. Thomas Harter. and Dr. Shahar Baram, Land, Air & Water Resources, UC Davis
Christine Stockert Land, Staff Research Associate, and Rebekah Davis, Junior Specialist, UC Davis

Objectives:

The overarching objective is to quantify and demonstrate the efficacy of irrigation water nitrogen (N) as a component of orchard N budgets ("pump and fertilize", P&F), and to contrast the P&F approach with "advanced grower practice" (split applications targeted to N demand and root proliferation, AGP) and high frequency low N concentration fertigation (HFLN). The objectives being pursued under this agreement include:

1) Establish research and demonstration orchards for "Advanced Grower Practice" (AGP) and "High Frequency Low Nitrogen Concentration" (HFLC, 'spoon feed') as contrasted with "Pump and Fertilize" (P&F) nitrogen (N) management in pistachio and/or almond within two "Hydrogeologically Vulnerable Areas" (HVAs)
2) Utilize and validate recent developments in yield and nutrient budget N management, early season sampling and yield estimation (AGP) to describe best management practices and contrast those practices with P&F N management treatments
3) Characterize key biological and physical parameters relevant to the P&F concept (concentration dependent uptake, root distribution and activity, phenology of uptake, seasonal plant-soil N balance, soil NO_3^- movement etc.)
4) Establish proof of concept for use of stable isotopes of $\delta^{15}N\text{-}NO_3^-$ in N tracing under P&F practices
5) Develop and grounds validate decision support models (including HYDRUS) to assist growers with optimal management of groundwater nitrogen (NO_3^-)
6) Demonstrate and proactively extend developed results, technologies relevant to on-site self-assessment and BMP's to growers

Interpretive Summary:

Over 30 million California residents (about 85%) rely partially or fully on groundwater as a source of drinking water (SWRCB, 2012). Nearly 2,600 California communities rely on about 8,400 community public supply wells as the main source of their drinking water. Among these, 1,662 public supply wells in 682 California communities are contaminated, and in one-third of these communities due to nitrate pollution alone (206 communities with 452 nitrate contaminated wells). This does not include private domestic households or households on state-small and local public water systems (2-14 connections), of which as many as 40% may be contaminated with nitrate (Boyle et al., 2012). In regions with predominantly agricultural land use, such as the Central Valley and the Salinas Valley, over 90% of groundwater nitrate pollution is estimated to originate from agricultural lands (Harter et al., 2012). Improved water and nutrient management practices would lead to significantly lower groundwater nitrate (NO_3^-) pollution. These practices must also account for non-fertilizer sources of nitrogen, such as irrigation water nitrogen and soil amendment nitrogen, (Dzurella et al., 2012). Few studies have considered managing nitrate in irrigation water ("pump and fertigate"), but in one example it was found that replacement of commercial fertilizer with irrigation water NO_3^- was effective at a 1:1 ratio or better (King et al., 2012). There is a need to develop an understanding of the utility of groundwater nitrate as a source of N for nut crops and to field demonstrate this practice so that guidelines for grower implementation can be developed and extended.

Our primary objective during the first half of 2015 was to continue monitoring leaching and N-mass balance for a second season under proposed best management practices by applying nutrient budget N management and to describe and contrast those practices with 'Pump and Fertilize' treatments. These experiments are continuing during the first half of 2016 for three seasons of data. Prior to the beginning of the growing season, the growers in all three orchards planned the N budget for the year based on the Almond Nitrogen Model accounting for groundwater NO_3^--N concentration (P&F). N-fertilizer was applied as planned and leaf samples indicated there was no need to modify the N-budget mid-season. During the 2015 growing season N-fertilizer (UAN 32) was applied at the end of irrigation/fertigation events while during 2014 it was applied in the middle of irrigation. Differences were observed in the temporal trends of the NO_3^--N concentrations at 180 cm and 290 cm (potential leachable NO_3^-) during 2014, 2015 and 2016 growing seasons. The observed differences in NO_3^--N showed that fertigation at the beginning/middle of an irrigation cycle tended to increase seasonal NO_3^- leaching, while fertigation events at the end of the irrigation cycle reduced the potential for NO_3^- leaching. Pre-bloom and post-harvest flood irrigation events led to deep wetting (>300 cm) and downward flushing of NO_3^--N deep into the vadose zone. Comparison between the total N loads in the soil profile based on soil extractions down to depth of 3 m prior to the beginning of the 2014, 2015 and 2016 growing seasons, suggested minimal, if any, N uptake from the deep profile (>1.5 m). Soil extraction indicated the persistence of high N-loads in the subsurface. Differences were observed between the soil extractions and the pore-water samples from similar sites, suggesting that there were two main N-phases in the soil, one mobile phase and another immobile. The differences between the two sampling methods indicated that most of the applied N-fertilizer stays in the mobile phase and therefore is more likely to propagate deep into the vadose zone and contaminate groundwater. Based on water mass balance of one orchard, the average leaching in the almond orchard over a growing season was 12±8 cm, and ranged from 0 to 24.5 cm. N-mass balance showed that during the

2014 growing season 95 – 152 and 44 – 52 lb.-N acre^{-1} were not accounted for in the almond and pistachio orchard, respectively. Based on the water and N mass balance, NO_3^--N concentrations in the water leaching below the almond orchard should be 89 – 142 mg/L. The statistical approach of principal component analysis (PCA) was used to evaluate the correlations between NO_3^--N concentrations at depth of 290 cm (427 water samples) and the principal factors that may influence it. In all the fertigation strategies (AGP, HFLC and P&F) NO_3^--N concentrations were positively correlated with the timing within an irrigation event of fertilizer injection and total length of irrigation. NO_3^--N concentrations were negatively correlated with the presence and thickness of hard pan in the subsurface and flood irrigation. The correlations emphasize the need for fertilizer application towards the end of an irrigation event, and the need for short term consecutive irrigations to keep the fertilizer and water in the active root zone (<1.5 m). The presence, depth and width of the hard pan, the time of fertigation and the length of the irrigation following the fertilizer injection had the highest contribution to explanation of variability in the data. These data highlight that it may be water management that is critical rather than any single proposed best management N practice.

Materials and Methods:

Objective 1. Establish research and demonstration orchards for P&F as well as AGP and HFLN N management in almond within two "Hydrogeologically Vulnerable Areas" (HVAs)

Three orchards were established in two HVAs, one located in the Madera groundwater basin between the Madera Water Bank (North) and the San Joaquin River (South), the municipality of Madera (East) and the San Joaquin River (West). Matt Andrew of ATB Growers, a cooperative that encompasses more than 2,100 acres of almond and pistachio, is the grower and contact person. Using ground water depth information taken from Department of Water Resources and Madera Irrigation District databases, we established two orchards (one pistachio, one almond) where the fertilizer strategies of AGP, P&F and HFLN were tested and contrasted during the 2014, 2015 and 2016 (almond) growing seasons. We have established fully randomized complete blocks designs for the two orchards, the orchard treatments were carried through to harvest in 2014, 2015 and 2016. Only the almond orchard treatments in the Madera sites will be carried through the 2016 growing season because of a grower error in the pistachio orchard.

We worked to identify and now work with a new grower in the Modesto Groundwater Basin. This represents a delayed component of the project and has involved an extensive search for a grower/cooperator within an HVA area consisting of 'shallow' depth to groundwater (e.g. 25-35 ft.) and sandy or sandy loam type soils. We anticipate conducting a soil survey and installing groundwater monitoring wells shortly after the 2016 harvest (September).

We have entered into initial agreement with the grower and we conducted a soil survey during September 2015 for proposed establishment of GW monitoring wells (**Figure 1**).

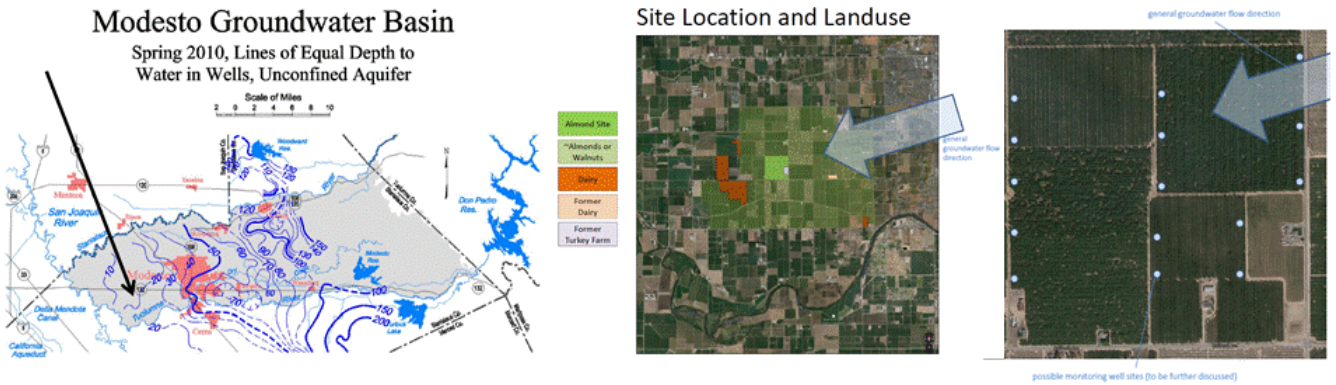

Figure 1: Location in the Modesto Groundwater Basin (A), land use patterns (B) and preliminary plan for network of groundwater monitoring wells (C) associated with continuous high frequency P&F fertilizer N management.

Objective 2. Utilize and validate recent developments in yield and nutrient budget N management, early season sampling and yield estimation to prescribe best management practices and contrast those practices with P&F nitrogen management treatments.

In each orchard eight sites were instrumented with an access tube for neutron probe, five root zone and deep solution samplers, four deep tensiometers, and five 5TE probes (Decagon, Pullman, WA, USA). The installed sensors monitor processes in and below the root zone. The depth at which the probes were installed were based on observation in three soil pits (3 m depth) excavated to determine rooting depth (**Figure 2**). Dositrons were installed at the high frequency subplots to facilitate nitrogen (N) additions, and a subcontract developed with Dr. Sharon Benes at Fresno State University to engage an irrigation management intern to work with grower/cooperators to insure N application amounts were accurate.

Objective 3. Characterize key biological and physical parameters relevant to the P&F concept (concentration dependent uptake, root distribution and activity, phenology of uptake, seasonal plant-soil N balance, soil NO_3^- movement etc.)

Nitrogen concentrations in the subsurface soils were estimated prior to and through the growing season. Nitrogen concentrations prior to the growing season indicated accumulation of NO_3^--N in the subsurface (>150 cm). The high concentrations in the deep profile below the root zone, suggested there is a risk for groundwater contamination by NO_3^- leaching. Data being processed for the current season and gathered during the upcoming season should reveal whether or not treatment differences exist among AGP, P&F and HFLN but there is not currently sufficient data to make any definitive statements.

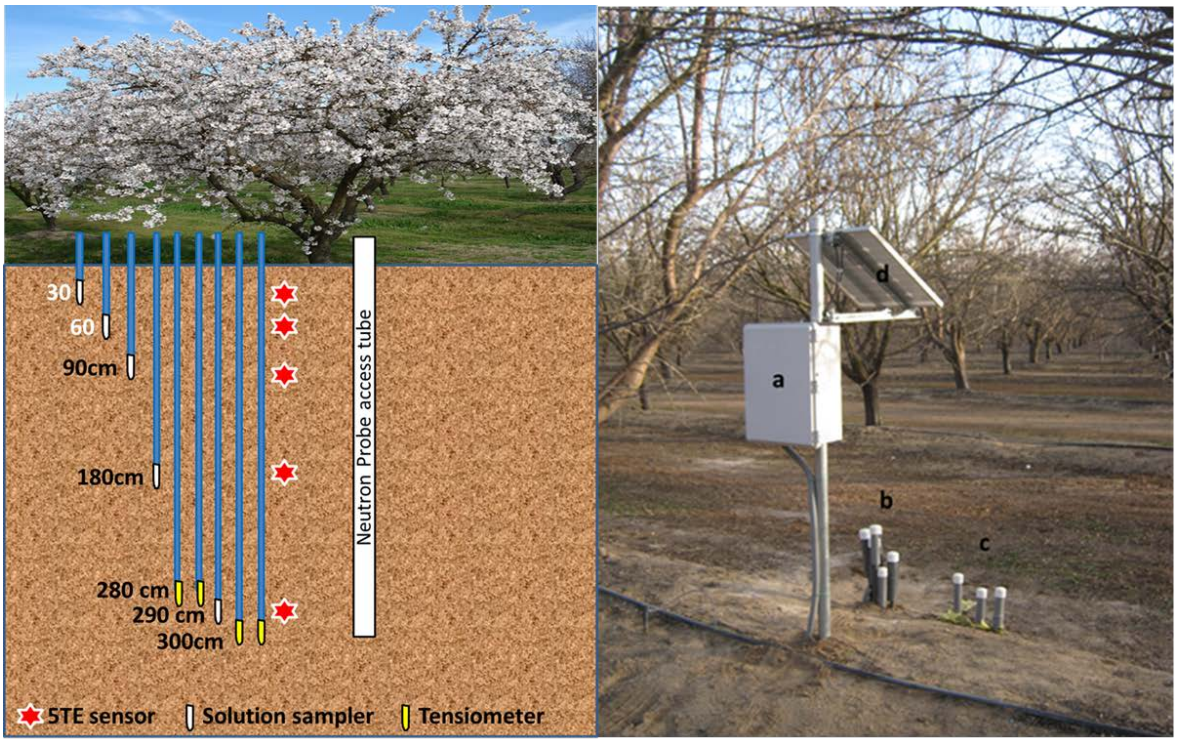

Figure 2: The basic set-up of the intensively monitored trees (left panel), and the way it appears in the almond orchard within Madera HVAI (right panel). (a) Housing for the electronics, (b) tensiometers and deep solution samplers (280 – 300 cm below land surface (bls)), (c) shallow solution samplers (30, 60, 90 cm bls), and (d) solar panel to charge the battery powering the electronics.

Objective 4. Establish proof of concept for use of stable isotopes of $\delta^{15}N\text{-}NO_3^-$ in N tracing under P&F practices.

To assess the $\delta^{15}N$ and $\delta^{18}O$ of nitrate (NO_3^-) in ground water and the vadose zone, the isotopic ratios of $^{15}N/^{14}N$ and $^{18}O/^{16}O$ are quantified by converting the solution NO_3^- into nitrous oxide (N_2O) in an oxygen free environment (zero grade N_2). N_2O in the head space then serves as the analyte for continuous flow gas chromatography (GC) isotope ratio mass spectrometry (IRMS). A culture of denitrifying bacteria (*Pseudomonas chlororaphis* and *P. aureofaciens*) is used in this headspace analysis for enzymatic conversion of NO_3^- to N_2O, which follows the reaction pathway shown in equation 1:

$$NO_3^- \rightarrow NO_2^- \rightarrow NO \rightarrow \tfrac{1}{2}N_2O \qquad \text{eqn 1}$$

Because the bacteria lack N_2O reductase activity, the reaction stops at N_2O, unlike most microbial denitrification reductions that go to completion at N_2. Once the conversion is complete, the zero grade N_2 containing microbially derived N_2O is extracted from the vial and separated from water vapor by an inline nafion membrane drier and from CO_2 with a layered $Mg(ClO_4)_2$/Ascarite trap. N_2O focusing is achieved by trapping the N_2O in a small-volume trap immersed in liquid nitrogen (-196°C). After the N_2O is warmed and released, it is purified by gas chromatography (GC) before being carried by helium to the IRMS via an Agilent GS-Q capillary column (30m x 0.32 mm, 40°C, 1.0 mL min^{-1}). This column separates N_2O from any residual CO_2. The IRMS is a continuous flow isotope-ratio mass spectrometer (CF-IRMS). It has a universal triple collector, consisting of two wide faraday cups with a narrower center cup

for quantifying ratios of 44:45, 44:46 and 45:46 N_2O. The ion beams from these *m/z* values are as follows: *m/z* = 44 = N_2O = $^{14}N^{14}N^{16}O$, *m*/*z* = 45 = N_2O = $^{14}N^{15}N^{16}O$ or $^{14}N^{14}N^{17}O$, and *m/z* = 46 = N_2O = $^{14}N^{14}N^{18}O$. The ^{17}O contributions to the *m*/*z* 44 and *m*/*z* 45 ion beams are accounted for before $\delta^{15}N$ values are reported.

Objective 5. Develop and ground validate decision support models (including HYDRUS) to assist growers with optimal management of groundwater nitrogen (NO_3^-).

The field gathered data on matric potential and water content from depths of 280 – 300 cm was used to generate in-situ retention curves for the deep soil at the different monitoring sites. RETC code (van Genuchten et al., 1991) was used with the parametrized models of van Genuchten (van Genuchten, 1980) to represent the soil water retention curve and the theoretical pore-size distribution models of Mualem and Burdine (Mualem, 1976) to predict the unsaturated hydraulic conductivity function from the gathered soil water retention data. The predicted unsaturated hydraulic conductivity parameters (α, n), along with the measured hydraulic gradient between 280 and 300 cm were used to calculate the daily unsaturated hydraulic conductivity (k(h)) and the Darcy flow equation to estimate the water flux below the root zone.

Results and Discussion:

Objective 2. Utilize and validate recent developments in yield and nutrient budget N management, early season sampling and yield estimation to prescribe best management practices and contrast those practices with P&F nitrogen management treatments.

Following the farmer's request, the research site at Turlock was not used in the 2016 growing season. Prior to the beginning of the growing season the nitrogen budget for the year was planned with the grower for the almond orchard using the Almond Nitrogen Model (Almond Nitrogen Model, 2014) and for the pistachio orchard using the work of Siddiqui and Brown (2013) (**Table 1**). The operation of a new deep groundwater pump at the Madera site In April 2015 decreased the irrigation water NO_3^- concentration from 35 to 9 mg L^{-1} (Smart et al., 2015). Accordingly, to get representative P&F treatment and duplicate the 2014 growing season, in the 2016 season NO_3^- has been added to the irrigation water as $Ca(NO_3^-)_2$ to get a concentration of 35 mg-NO_3^- L^{-1} in it. Irrigation water samples have been collected at the end of each irrigation event and, NO_3^- concentration in the irrigation water was analyzed to ensure that the concentrations resemble the 2014 NO_3^- concentrations. 'Dosatrons' were used to distribute the N-fertilizer loads according to seasonal uptake curve for almonds and pistachios (http://apps.cdfa.ca.gov/frep/docs/N_Almonds.html;http://apps.cdfa.ca.gov/frep/docs/N_Pistachio.html, respectively).

Table 1 summarizes the loads applied so far to the orchards at Madera. Leaf samples were collected in mid-April, as recommended by the Almond Nitrogen Model, and total nutrient analysis was performed. The analysis indicated that there was no need to adjust the N-budget (**Table 3**). At the almond orchard the grower applied most of the N-fertilizer earlier than planned, and with total N-load that is equivalent to an anticipated yield of 3000 lb.-kernel $acre^{-1}$, while the model predicted yield of 2648 lb.-kernel $acre^{-1}$ (**Table 1**). The HFLC treatment at

the pistachio site did not follow the planned schedule, due to miscommunication between us and the grower, and most of the fertilizer was applied early in the season (**Table 2**).

Table 1. Planned and applied N-fertilizer loads to the AGP and P&F subplots at the almond and pistachio orchards during the 2016 growing season

		AGP					P&F				
		Mar-Apr.	May-Jun.	Jun.-Jul.	Jul.-Aug.	Total	Mar-Apr.	May-Jun.	Jun.-Jul.	Jul.-Aug.	Total
Almond	Planned	69	92	69	0	230	48	64	48	0	161
	Applied	243	54	0		297	170	38	0		208
Pistachio	Planned	40	40	40	40	160	28	28	28	28	112
	Applied	39	47	47		128	39	43	33		115

Table 2. Planned and applied N-fertilizer loads to the HFLC subplots at the almond and pistachio orchards during the 2016 growing season

		HFLC				
		Mar-Apr.	May-Jun.	Jun.-Jul.	Jul.-Aug.	Total
Almond	Planned	48	64	48	0	161
	Applied	55	66			121
Pistachio	Planned	28	28	28	28	112
	Applied	53	57			110

Objective 3. Characterize key biological and physical parameters relevant to the P&F concept (concentration dependent uptake, root distribution and activity, phenology of uptake, seasonal plant-soil N balance, soil NO_3^- movement etc.)

Soil samples were collected at February 2016 to determine the N content in the soil prior to the beginning of the growing season. Three locations were sampled at each treatment (P&F, AGP, HFLC) at 30 cm intervals. The sediment was extracted on 1:1 ratio with 2M KCl solution. The concentrations were compared to the concentrations measured a year (2015) and two years earlier (2014) and indicated that the total N in the vadose zone did not change significantly between growing seasons (**Figure 3**).

From the initiation of the monitoring and up to date more than 1300 porewater samples have been collected from the soil profile under both orchards. From January 2016 through June 30 2016, 150 porewater samples were collected. Similar to the previous years, high spatial variability is still observed in the N concentrations along the orchard. Across all treatments NO_3^- concentrations ranged from lower than the drinking water standard (<10 mg-NO_3^--N L^{-1}) up to more than ten times the drinking water standard (**Figure 3**). Comparison between the temporal variability observed in the porewater N concentration and the soil extraction support our previous conclusions that despite the deep wetting following the flood irrigation, a significant immobile N pool remains and dominates the total N storage at 1.5 – 3.0 m soil depth (Baram et al., 2016; Smart et al., 2015).

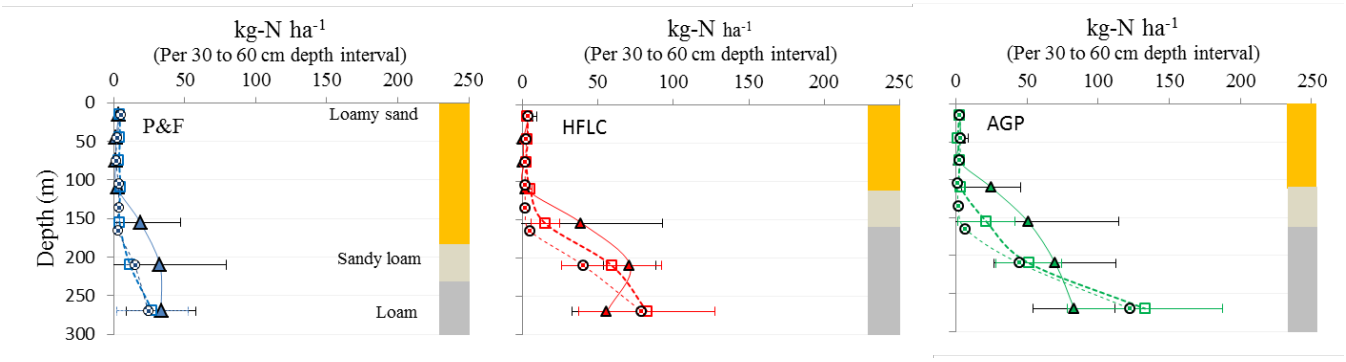

Figure 3. Nitrogen loads in the soil profile under the almond orchard in Madera at February 2014 (triangles), February 2015 (square) and February 2016 (circle). All the concentrations are normalized to the water content and presented as average of three sampling locations, with error bar presenting the standard deviation. The left, middle and right panels locations under the treatment; the panel represent locations under the P&F, HFLC and AGP treatments, respectively. The lithological profile at each site is presented at the right side of each panel.

In addition to the statistical methods reported by us in the past (Baram et al., 2016; Smart et al., 2015) which looked for correlations between the lithological profile and the fertigation regime, we analyzed the spatial variability of porewater NO_3^- concentration at depth of 2.9 m using semivariograms $\gamma(h)$ (Isaaks and Srivastava, 1990):

$$\gamma = \frac{1}{2N(h)} \cdot \sum_{i=1}^{N(h)} [z(x_i) - z(x_i + h)]^2 \qquad (1)$$

where h is the distance between two sampling sites (known as 'lag distance'), $z(x_i)$ is the measured NO_3^- concentration at site x_i and $N(h)$ is the number of pairs with the distance h. Using ArcGIS (Esri, 2011) kriging variogram model was fitted to the experimental variogram. The optimized semivariograms model found a lag distance of 8.5 m and indicated that the porewater NO_3^- concentration were spatially correlated up to a distance of 60 m (range = 60 m), yet with a fairly high root mean square error (RMSE ~50 mg NO_3^--N L^{-1}). In the model lag distance of 20, 50 and 100 m indicated range of 115-130 m (**Figure 4a**).

On top of the semivariogram method we wanted to see if the spatial variability in NO_3^- concentration increases with the distance between sampling points. For that purpose, coefficient of variation was calculated as the ratio between the standard deviation and the mean NO_3^- concentration for all the samples at a given distance (i.e. $N(h)$ and h). In all the calculations the yearly mean concentration at each one of the monitoring site was used. Over the orchard the coefficient of variation of NO_3^- concentration increased with distance between sites, up to a distance of 80 m where it remained at value of ~100%. On the local scale (up to 70 m between sites), similar trend of increased variance with distance was observed on one row (Site A), while on another row no trend was observed (Site B) and on a third row (Sites C) opposite trend was observed (**Figure 4b**). Both statistical methods, along with the methods previously reported (Smart et al., 2015), suggested that additional parameters not considered in this study, such as water application nonuniformity at the tree scale and sampling location relative to the emitters (Rolston et al., 1991), as well as spatial variations in root nutrient and water uptake rates within and between trees (Couvreur et al., 2016) and variation in yield and

N content in the kernels (Siddiqui and Brown, 2013; Silva et al., 2013) impacted N concentrations.

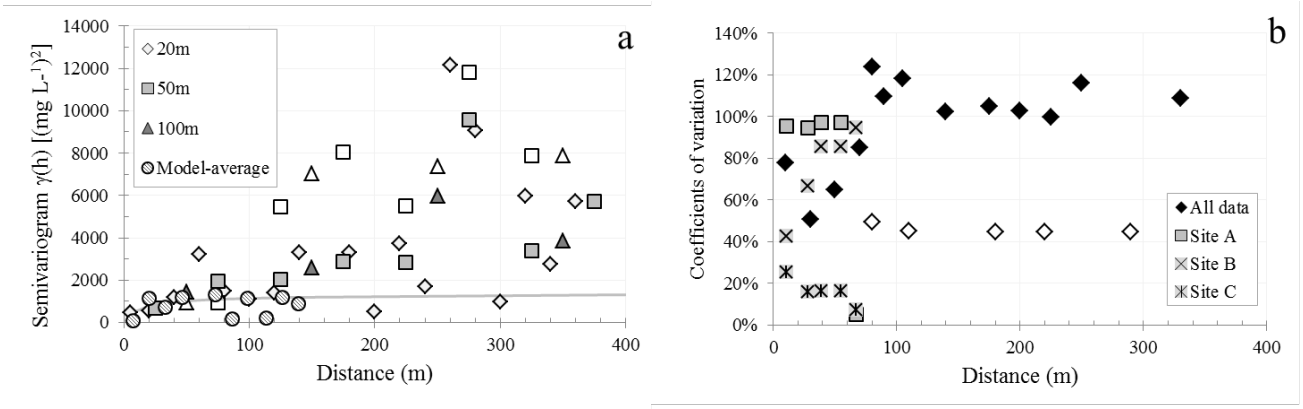

Figure 4. Semivariogram (a) and coefficient of variation (b) of NO_3^--N concentration in relation to the distance between the porewater sampling sites. Hallow and full symbols represent the 2014 and 2015 porewater NO_3^--N concentrations, respectively. Continuous gray line represents the optimized semivariogram predicted by ArcGIS.

Similar to previous years, the orchard was flood irrigated prior to bloom, which led to deep wetting and downward leaching (**Figure 5**) of water and NO_3^-. Following flood irrigation, from February through May, the soil profile down to 300 cm below the land surface dried, coinciding with a decrease in the hydraulic gradient between 280 and 300 cm (**Figure 5**). This is consistent with a management practice that is not quite amenable to diminishing NO_3^- leaching risk, and has been observed in the orchard over all the seasons we have participated, although in some cases the flood irrigation occurred in the fall following harvest (2014).

Objective 4. Establish proof of concept for use of stable isotopes of $\delta^{15}N$-NO_3^- in N tracing under P&F practices.

The isotopic studies were discontinued in 2015-2016 because sufficient data exists from the 2013-2015 seasons to answer the fundamental question concerning proof of concept. The data are highly consistent with tree uptake, or some other metabolic process, discriminating toward ^{15}N and thus analysis of natural abundance of ^{15}N ($\delta^{15}N$) and ^{18}O ($\delta^{18}O$) of N are not effective in determining a source. We currently have a manuscript in preparation that reviews our data and that of other researchers. NO_3^- stable isotopes of nitrogen ($\delta^{15}N$) and oxygen ($\delta^{18}O$) of NO_3^- in irrigation water and porewater, as compared with N of leaf and kernel samples indicated enrichment from depth of the porewater $\delta^{15}N$. The NO_3^- sampled from the subsurface indicated values higher than that of the groundwater. The $\delta^{15}N$ values of organic-N in the kernels did not vary between treatments and suggested uniform mixing of groundwater N with N from fertilizer among treatments.

Objective 5. Develop and ground validate decision support models (including HYDRUS) to assist growers with optimal management of groundwater nitrogen (NO_3^-).

In the first half of 2016 we focused on using the field gathered data to estimate the water flux and N losses through leaching below the root zone. We compared between three methods: (i) mass balance, (ii) Darcy method, and (iii) inverse modeling using Matlab and HYDRUS.

Provided here is a detailed description of the approach we used along with the results and conclusion.

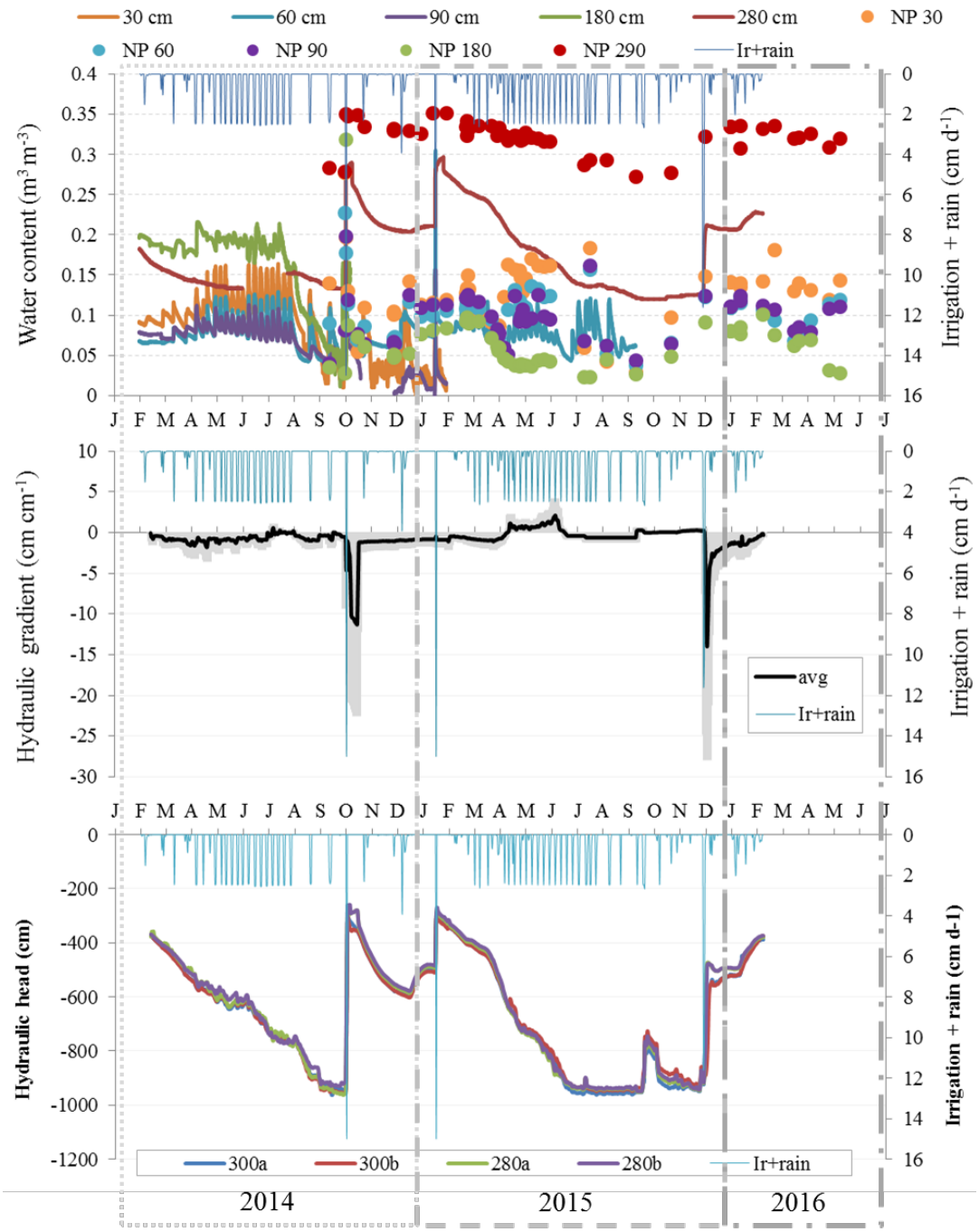

Figure 5. Changes over time in volumetric soil moisture content (C, θv) over the entire rooting zone gathered using 5TE sensors and neutron probe (NP) (upper panel) in average hydraulic gradient between 300 and 280 cm (middle panel) and in daily hydraulic head at 280 and 300 cm below land surface (lower panel).

1. *Mass balance* – In the mass balance method, the annual N mass lost through leaching (*M*), was calculated using the equation:

$$M = \sum_{i=1}^{12} V_i C_i \qquad (1)$$

where *V* is the volume of water leaching every month (*i*) below 3 m soil depth (m^3), *C* is the average N concentration in the leaching water at that depth during that month (g m^{-3}). The volume of water leaching below 3 m soil depth was calculated for each site using:

$$L = (Ir+rain) - (ET_c) - (\Delta S) \qquad (2)$$

$$V = LA \qquad (3)$$

where *L* is the weekly water leaching flux (cm $week^{-1}$), *Ir* and *rain* are the cumulative weekly irrigation and precipitation, respectively (cm $week^{-1}$), ET_c is the cumulative weekly water loss through evapotranspiration (cm $week^{-1}$), ΔS is the change in soil water storage over a week (cm $week^{-1}$) and *A* is a hectare (10,000 m^2). ΔS was calculated both based on 5TE data and NP data. In the 5TE based storage calculations the lithological profile was accounted for. ET_c was estimated based on ET_o data from California Irrigation Management Information System – Station No.188 (CIMIS 2014), which was multiplied by crop coefficients (K_c) based on the work of Goldhamer (2012).

2. *Darcy Method* – In this method, the leaching flux below a depth of 3 m was calculated daily using the empiric law of Darcy:

$$q = K\frac{\partial h}{\partial z} \qquad (4)$$

where *q* is the leaching flux (cm d^{-1}), *K* is the hydraulic conductivity (cm d^{-1}), *h* is the total hydraulic head (cm) and *z* is the elevation above a vertical datum (cm). The hydraulic conductivity was calculated daily as a function of the matric potential ($K(\psi)$) using the van Genuchten (1980) Mualem (1976) formula:

$$K(\psi) = K_s\left(\frac{1}{\left[1+(\alpha|\psi|)^n\right]^{1-\frac{1}{n}}}\right)^{\frac{1}{2}}\left[1-\left(1-\left(\frac{1}{\left[1+(\alpha|\psi|)^n\right]^{1-\frac{1}{n}}}\right)^{\frac{n}{n-1}}\right)^{1-\frac{1}{n}}\right]^2 \qquad (5)$$

where K_s is the hydraulic conductivity at saturation (cm d^{-1}), ψ is the matric potential (cm) and α (cm^{-1}) and *n* (–) are empirical parameters which are related to the inverse of the air entry pressure and the pore-size distribution, respectively. The field gathered matric potentials at depths of 2.8 and 3.0 m data and the water content at depth of 2.9 (5TE and the NP), were used to generate eight in-situ retention curves for each monitoring site and

RETC code (van Genuchten et al., 1991) was used to fit the α and *n* parameters for each curve to get the daily *K(ψ)* (Eq. 5) (**Figure 6**). K_s of the soils at depth of 2.8 m in each site were estimated using the permeameter method. K_s was calculated using (U.S. BR-DO-MEB, 1990):

$$K_s = \frac{Q}{2\pi h^2}\left\{\ln\left[\frac{h}{r}+\sqrt{\left(\frac{h}{r}\right)^2+1}\right]-\left[\frac{\sqrt{\left(\frac{h}{r}\right)^2+1}}{\frac{h}{r}}\right]+\frac{1}{\frac{h}{r}}\right\} \qquad (6)$$

where *Q* is steady flow rate (ml s^{-1}), *h* is height of constant water head in the borehole (cm), *r* is borehole radius (cm) and *π* is 3.14. Similar to the mass balance method, nitrogen leaching below the root zone was calculated daily using equations 1 and 3, where *L* is substituted by *q*.

3. *Inverse Modeling Framework Methodology* – The HYDRUS code (Šimůnek et al., 1998) along with MATLAB software (MathWorks, 2012) were used as an inverse modeling framework to estimate water leaching and NO_3^- transport at soil depth of 3 m. In the inverse modeling, field gathered data of soil water content, soil matric potential, and their temporal changes was used as observation points. The field gathered data was first used in an optimization program that combined the Genetic Algorithm (GA) global optimizer and the FMinSearch and FMinCon local optimizers (available in MATLAB) (for more information on the optimizer see Coleman and Li (1996), Lagarias et al. (1998) and Whitley (1994)). In the optimization process the program incorporated effective hydraulic properties to soil horizonation. The optimization process used an initial population of parameter sets ('P') which was randomly picked from a defined and bounded parametric space (Table 4). Once the initial parameters were picked (i.e. four parameters of van Genuchten (1980) equation: water content at saturation – θs, α, n and Ks, assuming m = 1-1/n.), the Richards' flow equation (Richards, 1931) was solved in HYDRUS coupled with Feddes et al. (1978) root water uptake model (using: h2 = –600 cm, h3 = –8000 cm and ωc = 0.3) and Vrugt et al. (2001) one-dimensional root distribution model (z* = –10 cm, z0 = –145 cm and pz = 0 (linear)) models.

   For each tested parameter set, differences between simulated and measured observations were quantified with a second-order moment of residuals, which gives more weight to large errors in the objective function (i.e. squared errors). Those residuals were then averaged; uniform weights were attributed to different observations of the same type for local water content, total water storage and matric potential. Temporal changes of water content and storage were considered as separate observations, which were attributed weights proportional to their amplitude (i.e. large changes have more weight). Average water status was used to normalize the average residuals. The normalization enabled to aggregate the different error types, with no effect of their units, into a single non-dimensional value. The aggregated value was than stored, and a new set of parameters P was picked from the parametric space, using either global or local optimizer. The optimizers kept on looking for new P values in the parametric space until the aggregated value of the objective function

reached the minimal value (i.e. best fit). Local optimizers were run after the global optimizer to refine the solution locally. In the optimization process, the residuals were calculated in a time frame of 8 – 12 months out of the 24 months of data. Extra observations were used for validation of the optimized parameters.

Table 3. Parametrization space limits used in the optimization

Parameter	Min-limit	Max-limit
θr (cm cm^{-1})	0.0	0.2
θs (cm cm^{-1})	0.2	0.34
$log_{10}(\square)$(cm^{-1})	-3	-1
n (-)	1.15	3.10
$log_{10}(\square s)$ (cm d^{-1})	-0.5	2.5

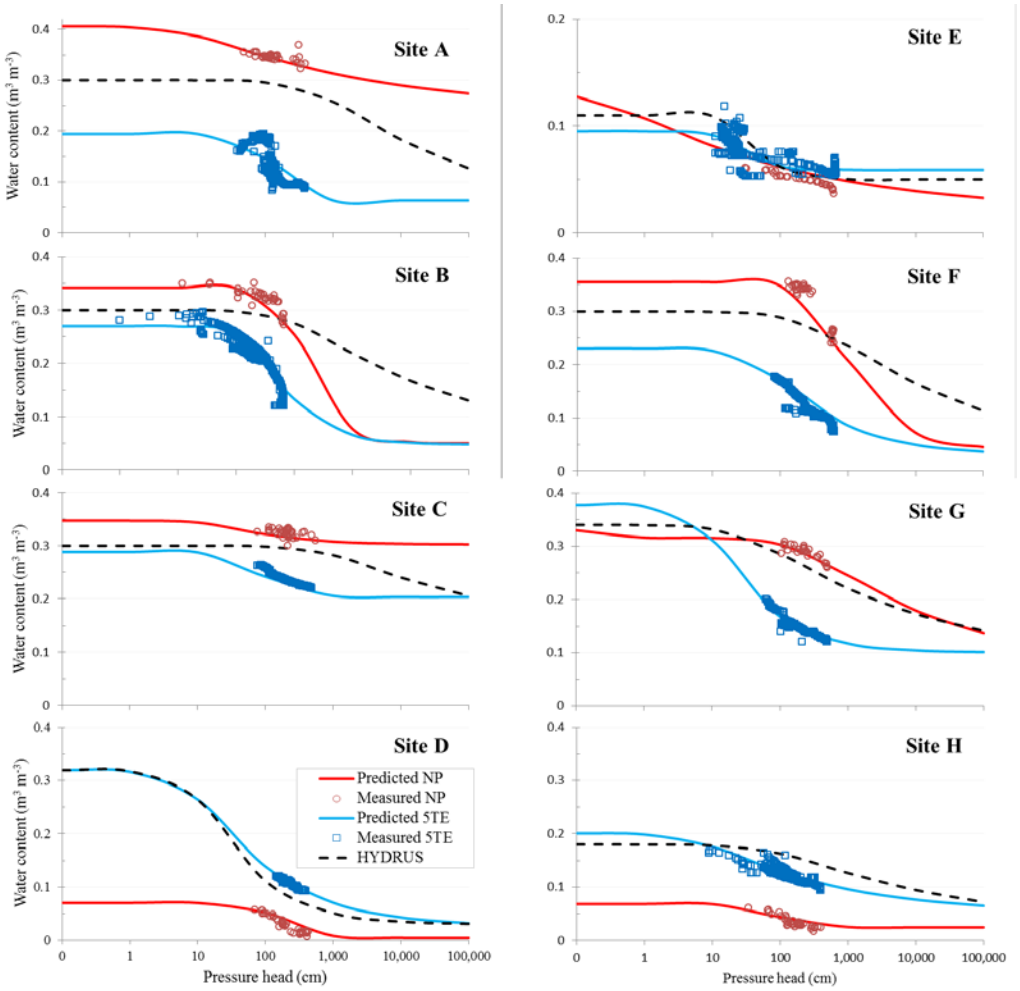

Figure 6. Retention curves for the soils at depth of 2.8 – 3.0 m based on 5TE, NP and tensiometers data from the eight vadose zone monitoring sites.

In all the simulations the top boundary conditions of precipitation and irrigation were based on field measurements, while evapotranspiration was defined based on ET_o data from CIMIS combined with *Kc* parameters of Goldhamer (2012) to transition linearly from the low plateau (*Kc1*) to the high plateau (*Kc2*), yearly. The monitored matric potentials and water contents were used to generate the initial soil matric potential profile. Initial matric potentials in-between observation depths were linearly interpolated. In the modeling, the continuous in-situ water content measurements of the 5TE sensors at each site were linearly correlated to the NP measurements from the corresponding depth at each site. The correlation factor for each site ($R^2 > 0.75$) was then used to convert the 5TE measurements to continuous NP water content measurements.

All three methods (i.e. mass balance, Darcy-flux and HYDRUS modeling) indicated high downward flux during the winter and early spring (December through late April), especially following flood irrigation events. Latter in the season (May through October) the soil profile dried and the downward flux approached zero (less negative) and even became positive, indicating upward water flux (**Figure 7a**). In 2014 the calculated average cumulative flux greatly varied between the three methods (12.0 – 32 cm y^{-1}), while in 2015 all the methods indicated more similar fluxes (12.6 – 22 cm y^{-1}) (**Figure 7b**). We believe that the upward flow fluxes calculated in the mass balance approach are inaccurate, due to the dry conditions which prevailed in the subsurface from May through October (ψ < -150 cm) and the corresponding calculated low hydraulic conductivities ($K(\psi)$ < 0.001 cm d^{-1}). Nonuniformity in the wetting patterns of the micro-sprinklers in the field (most of the water falls 1.8 – 2.4 m away from the sprinkler, field observations) generates conditions in which only part of the infiltrating irrigation water is captured by water content sensors. Accordingly, as the soil profile dries the difference between the applied water and the observed change in storage (ΔS) increases. In order to sustain the mass balance, water needs to enter the upper soil profile (< 3 m) from its bottom boundary (> 3 m) as upward water flux (Eq. 2). Differences between the orchard average ET_c values (Et_0 x *Kc*) and the actual ET value at the monitored trees are another driver for the unrealistic upward flow values. This assumption is strengthen by the work of Couvreur et al. (2016) that showed 5–8% spatial variations in root water uptake rates within and between trees in an almond orchard.

Darcy flux calculations showed that the yearly average fluxes below 3 m soil depth at the orchard, based on 5TE data and on NP data, were fairly similar (2014: 12.0 vs. 14.9 cm y^{-1}, respectively; 2015: 12.6 vs. 18.7 cm y^{-1}, respectively). In both growing seasons the water flux across the orchard remained in the same range (1 – 33 cm y^{-1}). However, up to 3 fold differences were observed between the flux calculated at each site based on 5TE and NP data. Similar to the Darcy method, the yearly average fluxes calculated based on the mass balance approach (Eq. 2) and NP and 5TE data were comparable (18.3 vs. 15.1 cm y^{-1}). Moreover, same differences (up to 3 fold) were observed between the fluxes calculated based on 5TE and NP data at each sites. In both methods, big differences were observed between the 5TE and NP based fluxes at Site-E (15 – 20 vs. 0.35 – 1.0 cm y^{-1}, respectively). The differences between the 5TE and NP base calculations are an outcome of the differences between the readings of the two methods, which results from two major factors: (i) soil volume measured by the sensor and, (ii) installation procedure. The soil volume measured by the 5TE sensor (0.0007 m^3; Decagon-Devices, 2016) is 20 – 700 times smaller than the volume measured by the NP (0.014 to 0.5 m^3; Robinson et al., 2008). In addition to the much smaller

volume measured by the 5TE sensor, it is difficult and sometimes impossible to properly install it at depth of 2.9 m (i.e. push the whole length of its semi-flexible brittle prongs into undisturbed sediment at the side wall of a borehole). It is therefore more reasonable to assume that NP readings, which sample a much larger area of undisturbed soil profile, are more representative of the 'true' water distribution in the subsurface, especially in deep vadose zone, as suggested by Yao et al. (2004). However, at an orchard scale the need for an operator and relatively slow data acquisition process makes it very hard to use NP as a tool to study the temporal dynamics (minutes to hours) of water along the vadose zone, especially over long periods; data that is easily acquired by sensors such as the 5TE when connected to data loggers.

The main limitation to the Darcy flux estimates came from its independence from mass balance conservation constraints. Accordingly, in three out of the eight monitoring sites, the field measured saturated hydraulic conductivities (K_s) had to be lowered by up to two orders of magnitude, in order to make sure that the drained flux did not exceed the applied water (especially following flood irrigation events). In all cases the corrected K_s values were in the range expected for the specific soil type (Clapp and Hornberger, 1978). One exception to that trend was observed in the K_s value for the 5TE measurements at Site E, where K_s value was lower by at least one order of magnitude than the expected value. We believe that this deviation is a result of the installation procedure of the 5TE sensor at that site, where fine sediment fell down into the borehole during the installation, and increased the water content values compared to undisturbed sediment. Overall the generation of in-situ retention curve, and its applicability in calculating the leaching flux based on monitoring of the hydraulic conditions in the vadose zone (matric potential and/or water content) is very accurate and is not biased by the uncertainty associated with tree scale ET assessments. However, care must be taken to make sure that the leaching values are constrained by mass balance conservation.

The monthly water fluxes calculated by the model were in good agreement with the fluxes calculated by the other methods (**Figure 8a**). Nonetheless, through most of the year the orchard average monthly flux calculate by the model was slightly higher than the flux calculated by the other methods, resulting in higher cumulative flux (**Figure 8b**). Similar to the other methods, very high fluxes were observed in Site E during the 2014 and 2015 growing seasons (56 and 30 cm y^{-1}, respectively). The range of fluxes calculated by the model for the different sites was smaller than the range in the other methods (2014: 22 – 30 cm y^{-1}, excluding Site E; 2015: 15 – 36 cm y^{-1}).

Unlike the two aforementioned methods, the HYDRUS modeling approach taken by us was constrained by both mass balance and hydraulic properties of the soil profile. Distinct to the Darcy method, where the hydraulic properties of the soil layer at depth of 2.8 – 3.0 m were characterized, the model optimization process fitted the field gathered data to get the hydraulic properties of two general soil layers of high and low permeability. In most cases the retention curves from the HYDRUS fitted parameters were less steep than the RETC predicted ones, indicating higher leaching potential at the low matric potentials for the model (**Figure 7**). The good agreement between the annual water losses, calculated based on the HYDRUS model and the Darcy method, suggests that the use simple root water uptake model (Feddes et al., 1978) and one-dimensional root distribution model (Vrugt et al., 2001) in addition to the Richards' flow equation was sufficient to capture the water flow dynamics at the different sites.

The orchard average NO_3^- fluxes below the effective root zone, across measuring and calculation methods were all in the same order of magnitude (80 – 240 kg-N ha^{-1} y^{-1}). In most sites Darcy flux calculations with 5TE data had the lowest NO_3^- fluxes, while mass balance calculations had the highest flux (**Figure 8**). In both growing seasons, no correlation was observed between the water flux at depth of 2.9 m and the mobile porewater NO_3^- concentration at that depth (R^2 = 0.017); that is: sites with high water flux did not have low porewater NO_3^- concentration, or vice versa. Based on the work of Baram et al. (2016) which showed that the N load in the soil at that research site did not change significantly between the two growing seasons, the orchard average annual N accumulation (applied – removed) served as good reference for the maximal load available annually for leaching. Nonetheless, the differences in N removal at the tree/row scale, suggest high spatial variability in N-accumulation within the orchard. The work of Silva et al. (2013) which studied multiple almond orchards for four years, shows similar variability in yield and N contents. This spatial variability may explain the high spatial variability in porewater NO_3^- concentration at depth of 2.9 m (**Figure 9**) and the differences between the annual N losses at the different monitoring sites (**Figure 8**).

The good agreement between the annual N accumulation and the vadose zone based estimates of N losses below the effective root zone indicates that at this research site, eight vadose zone monitoring sites, representing different soil layering, were sufficient to capture the spatial variability in N losses at the orchard scale. The conversed research site represents orchard management in which pre bloom fill of the soil water storage leads to leaching mainly early in the growing season when the soil profile is wet (February through early May). This management practice prevents long term N buildup in the subsurface, and also leads to increased N losses during early season fertilizer applications (Baram et al., 2016). In orchard where minimal leaching occurs, N would probably buildup in the subsurface, similar to the natural buildup of N in arid/semiarid regions (Stone and Edmunds, 2014). Accordingly, at such sites porewater sampling below the effective root zone may not represent the annual N-buildup, as observed under the pistachio orchard. Based on the spatial variability of the soil layering at the orchard scale, it is hard to determine whether eight vadose zone monitoring sites would be stuffiest to capture the spatial variability in N and water losses under different orchards. Indication to the limitation of predetermined number of soil sampling sites to represent mean field NO_3^- content was presented by Ilsemann et al. (2001).

Although the annual N losses can be estimated based on mass balance and vadose zone data, our results indicate that it is harder to estimate the orchard average NO_3^- concentration in the porewater leaching below the effective root zone. Using simple mass balance of N and water [(N-applied – N-removed)/(Rain + irrigation – ET_c)] indicates that the NO_3^--N concentrations in the leaching water should have been 38 and 143 mg L^{-1}, for the 2014 and 2015 growing seasons, respectively (**Table 1**). 2016 amounts are currently being calculated. At the same time, when annual N accumulation, is divided by the annual leaching estimated by water mass balance (Eq. 2), Darcy method (Eq. 4) and HYDRUS modeling, NO_3^--N concentrations in the leaching water should have been in the range of 82-43 and 66-45 mg L^{-1}, respectively. These NO_3^--N concentrations are lower than the orchard average concentration based on porewater sampling (109 and 75 mg L^{-1}, respectively). The big difference between calculated orchard average porewater NO_3^--N concentrations and the concentration in the sampled porewater probably stems from spatial variability in N uptake under uniform N

applications along with the dominance of preferential flow and N-transport at the orchard scale (Baram et al., 2016; Onsoy et al., 2005; Russo et al., 2014). Identification and quantification of high/low productivity zones within an orchard may be used to improve N losses estimates, as previously suggested by Delgado et al. (2005) for irrigated corn fields. Nonetheless, this problem did not fully prevent us from estimating a site specific monthly (**Figure 7**, cm water month^{-1}) and annual (**Figure 8**) leaching flux (kg N ha^{-1} yr^{-1}) from each site using a host of methodological approaches and that the mass balance approach has validated usefulness.

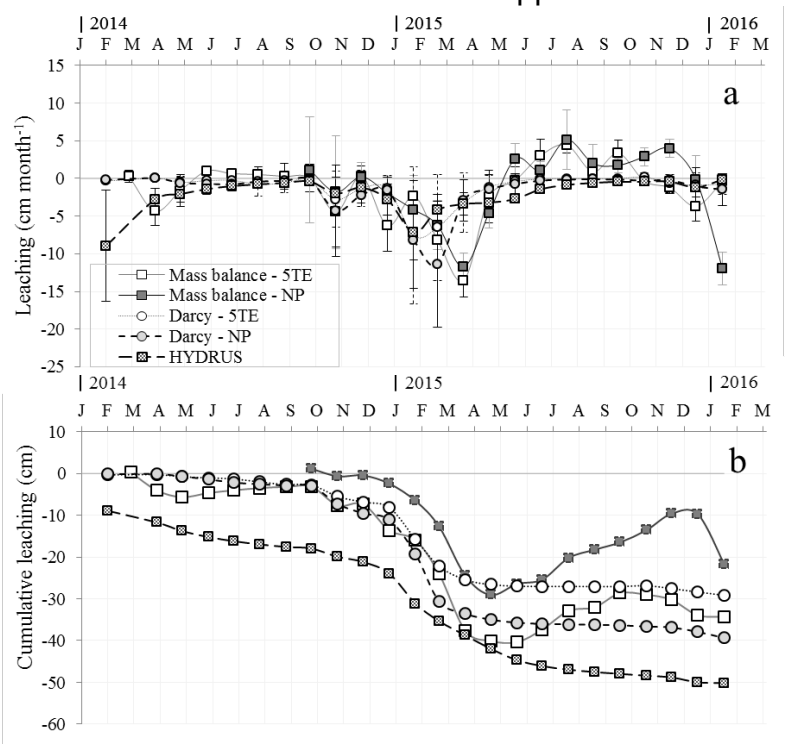

Figure 7. Average monthly leaching flux (a) and cumulative flux (b) at soil depth of 3 m calculated based on in-situ vadose zone data using mass balance, Darcy flow equation and HYDRUS modeling.

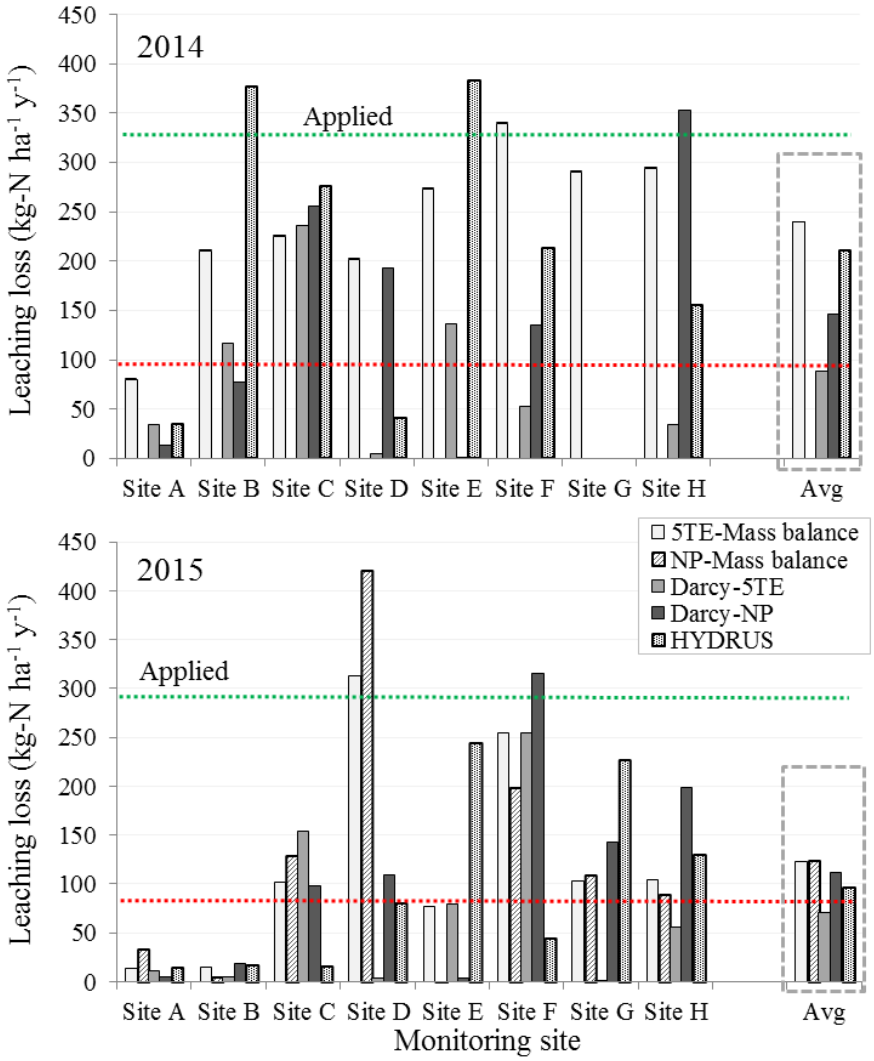

Figure 8. Yearly NO_3^--N leaching losses below soil depth of 3 m under the monitored sites and the orchard average for the three different methods (mass balance, Darcy flow and HYDRUS inverse modeling). Upper and lower dotted lines in each panel represent the N-load applied and the annual N accumulation, respectively.

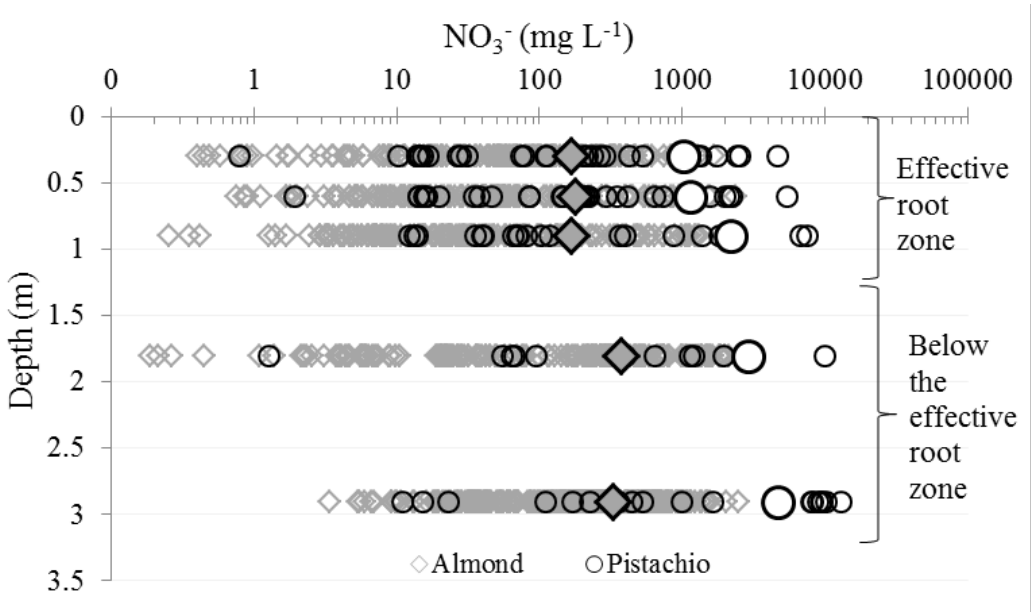

Figure 9. Nitrate concentrations in pore water samples taken throughout the monitoring period 2014 – 2016.

Objective 6. Demonstrate and proactively extend developed results, technologies relevant to on-site self-assessment and BMP's to growers.

The following represents a partial list of outcomes achieved by attending grower meetings and publishing or presenting proceedings/posters/advisories in conjunction with the meetings. These presentations are ongoing and will continue at the Almond Board of California (ABC Conference on December 6th to 8th 2016.

Schellenberg, DL, MW Wolff, MM Alsina, CM Stockert and DR Smart (2013) Net Primary Productivity and Greenhouse Gas Exchanges for Major California Perennial Crops. Farming for the Future: California Climate and Agriculture Summit, February 21st, California Climate Action Network (Cal-CAN), Davis, CA, >200 attendees.

Smart, DR, PH Brown, G Ludwig (2013) Nitrogen Use Efficiency of California Almond Orchards, USDA Central Valley Nitrogen Efficiency Conference, June 6th, Modesto CA, 40+ attendees.

Wolff, MW, DL Schellenberg, A Olivos, BL Sanden, PH Brown and DR Smart (2013) Reducing Mobile-N Loss from Fertigation: Field and Modeling Approaches. Improving Nitrogen Use Efficiency in Crop and Livestock Production Systems, Soil Science Society of America, August 13-15, Kansas City MO, >200 attendees.

Salas, W, DR Smart, J Kimmelshue (2013) DNDC Modeling Update, Sustainability Strategic Meeting, Oct 31st, 12 attendees.

Smart, DR (2013) Mitigation of Reactive N Mobilization (N_2O and NO_3^-) Using Injected, High Frequency Low Nitrogen Fertigation (HFLN). Almond Board of California Annual Meeting, Dec 3rd-5th, Sacramento CA, 2,555 attendees.

Smart DR (2013) Optimizing the Use of Ground Water Nitrogen in Nut Crops. Almond Board of California Annual Meeting, Dec 3rd-5th, Sacramento CA, 2,500+ attendees.

Smart, DR (2013) Mitigation of Reactive N Mobilization (N_2O and NO_3^-) Using Injected, High Frequency Low Nitrogen Fertigation (HFLN). Almond Board of California Annual Meeting Proceedings/Research Updates.

Smart DR (2014) Sustainable Management of the Root Zone, Sustainable Agriculture Expo, San Luis Obispo CA November 17-18th, >400 attendees.

Baram S, M Read, CM Stockert, T Harter, P Brown, JW Hopmans DR Smart (2014) Optimizing the Use of Groundwater Nitrogen (NO_3^-): Efficacy of the Pump and Fertilize Approach for Almond. Almond Board of California Annual Meeting, Dec 9th-11th, Sacramento CA, 2,925 attendees.

Smart, DR, S Baram, M Read, CM Stockert, T Harter, P Brown, JW Hopmans, (2014) Optimizing the Use of Groundwater Nitrogen (NO_3^-): Efficacy of the Pump and Fertilize Approach for Almond. Conference Proceedings/Research Updates.

Dabach, S, DR Smart, M Read, C Stockert (2014) Evaluating Nitrogen Management Strategies to Minimize Greenhouse Gas Emissions from California Almond Orchards. Almond Board of California Annual Meeting, Dec 8-10th, 2,925 attendees.

Smart, DR, S Dabach, M Read, C Stockert (2014) Evaluating Nitrogen Management Strategies to Minimize Greenhouse Gas Emissions from California Almond Orchards. Almond Board of California Annual Conference Proceedings/Research Updates.

Smart, DR, S Baram, M Read, CM Stockert, T Harter, P Brown, JW Hopmans, (2015) Optimizing the Use of Groundwater Nitrogen (NO_3^-): Efficacy of the Pump and Fertilize Approach for Almond. Conference Proceedings/Research Updates. >2,000 attendees

Dabach, S, DR Smart, M Read, C Stockert (2015) Evaluating Nitrogen Management Strategies to Minimize Greenhouse Gas Emissions from California Almond Orchards. Almond Board of California Annual Meeting, Dec 8-10th, >2,000 attendees.

DR Smart 2015. Optimizing the Use of Groundwater Nitrogen for Nut Crops. Western Plant Health Association, CDFA Fertilizer Research & Education Program, November 4th – 5th Seaside CA USA. >400 attendees

References:

Baram, S., Couvreur, V., Harter, T., Read, M., Brown, P.H., Hopmans, J.W. & Smart, D.R. (2016). Assessment of orchard N losses to groundwater with a vadose zone monitoring network. *Agricultural Water Management* 172:83–95.

Clapp, R.B., Hornberger, G.M., 1978. Empirical equations for some soil hydraulic properties. Water Resour. Res. 14, 601–604. doi:10.1029/WR014i004p00601

Coleman, T.F., Li, Y., 1996. An Interior Trust Region Approach for Nonlinear Minimization Subject to Bounds. SIAM J. Optim. 6, 418–445.

Cote, C. M., Bristow, K. L., Charlesworth, P. B., Cook, F. J., & Thorburn, P. J. (2003). Analysis of soil wetting and solute transport in subsurface trickle irrigation. *Irrigation Science*, *22*(3-4), 143–156. doi:10.1007/s00271-003-0080-8

Couvreur, V., Kandelous, M.M., Sanden, B.L., Lampinen, B.D., Hopmans, J.W., 2016. Downscaling transpiration rate from field to tree scale. Agric. For. Meteorol. 221, 71–77. doi:10.1016/j.agrformet.2016.02.008

Dzurella, K. N., Pettygrove, G. S., Fryjoff-Hung, A., Hollander, A., & Harter, T. (2015). Potential to assess nitrate leaching vulnerability of irrigated cropland. *Journal of Soil and Water Conservation*, *70*(1), 63–72. doi:10.2489/jswc.70.1.63

Delgado, J.A., Khosla, R., Bausch, W.C., Westfall, D.G., Inman, D.J., 2005. Nitrogen fertilizer management based on site-specific management zones reduces potential for nitrate leaching. *Journal of Soil and Water Conservation*, 60, 402–410.

Feddes, R.A., Kowalik, P.J., Zaradny, H., 1978. Simulation of Field Water Use and Crop Yield. Simulation Monograph.Pudoc, Wageningen, Netherlands.

Gärdenäs, A. I., Hopmans, J. W., Hanson, B. R., & Šimůnek, J. (2005). Two-dimensional modeling of nitrate leaching for various fertigation scenarios under micro-irrigation. *Agricultural Water Management*, *74*(3), 219–242. doi:10.1016/j.agwat.2004.11.011

Goldhamer, D., 2012. Almond in Group Yield Response to Water, in: Steduto, P., Hsiao, T.C., Fereres, E., Raes, D. (Eds.), FAO Irrigation and Drainage Paper No.66. Food and Agriculture Organization of the United Nations, Rome, Italy, p. 246:296.

Ilsemann, J., Goeb, S., Bachmann, J., 2001. How many soil samples are neccessary to obtain a reliable estimate of mean nitrate concentrations in an agricultural field? J. Plant Nutr. Soil Sci. 164, 585. doi:10.1002/1522-2624(200110)164:5<585::AID-JPLN585>3.0.CO;2-M

Isaaks, E.H., Srivastava, M.R., 1990. Applied geostatistics, Oxford University Press. Oxford University Press, New York.

Lagarias, J.C., Reeds, J.A., Wright, M.H., Wright, P.E., 1998. Convergence Properties of the Nelder--Mead Simplex Method in Low Dimensions. SIAM J. Optim. 9, 112–147. doi:10.1137/S1052623496303470

Mualem, Y. & A.P Bodine (1976). A new model for predicting the hydraulic conductivity of unsaturated porous media. *Water Resources Research*, *12*, 513–522. Retrieved from https://hwbdocuments.env.nm.gov/Los Alamos National Labs/TA 54/11570.pdf.

Onsoy, Y.S., Harter, T., Ginn, T.R., Horwath, W.R., 2005. Spatial variability and transport of nitrate in a deep alluvial vadose zone. Vadose Zone Journal, 4, 41–54.

Phogat, V., Mahadevan, M., Skewes, M., & Cox, J. W. (2011). Modelling soil water and salt dynamics under pulsed and continuous surface drip irrigation of almond and implications of system design. *Irrigation Science*, *30*(4), 315–333. doi:10.1007/s00271-011-0284-2.

Richards, L.A., 1931. Capillary conduction of liquids through porous mediums. Physics (College. Park. Md). 1, 318. doi:10.1063/1.1745010

Robinson, D.A., Campbell, C.S., Hopmans, J.W., Hornbuckle, B.K., Jones, S.B., Knight, R., Ogden, F., Selker, J., Wendroth, O., 2008. Soil Moisture Measurement for Ecological and Hydrological Watershed-Scale Observatories: A Review. Vadose Zo. J. 7, 358. doi:10.2136/vzj2007.0143

Rolston, D.E., Biggar, J.W., Nightingale, H.I., 1991. Temporal persistence of spatial soil-water patterns under trickle irrigation. Irrig. Sci. 12, 181–186. doi:10.1007/BF00190521

Russo, D., Laufer, A., Gerstl, Z., Ronen, D., Weisbrod, N., Zentner, E., 2014. On the mechanism of field-scale solute transport: Insights from numerical simulations and field observations. Water Resources Research, 50, 7484–7504. doi:10.1002/2014WR015514

Siddiqui, M.I., Brown, P., 2013. Pistachio Early-Season Sampling and In-Season Nitrogen Application Maximizes Productivity, Minimizes Loss; Protocol for Early-Season Sampling and In-Season Nitrogen Budgeting [WWW Document]. URL http://fruitsandnuts.ucdavis.edu/files/165545.pdf (accessed 8.29.15).

Silva, S.S., Saiful, M., Sanden, B., Laca, E., Brown, P., 2013. Almond Early-Season Sampling and In-Season Nitrogen Application Maximizes Productivity, Minimizes Loss - Protocol for Early-Season Sampling and In-Season Nitrogen Budgeting.

Simunek, J., Sejna, M., van Genuchten, M.T., 1998. The HYDRUS- 1D software package for simulating the one-dimensional movement of water, heat, and multiple solutes in variably saturated media. IGWMC-TPS-70,.

Smart, D.R., Dabach, S., Jerzurki, D. & Stockert C. (2015). Response of N_2O emissions and concentration profiles to irrigation method and implications for upscaling measured emissions in an almond orchard. *Agriculture and Forest Meteorology* (submitted)

Stone, A.E.C., Edmunds, W.M., 2014. Naturally-high nitrate in unsaturated zone sand dunes above the Stampriet Basin, Namibia. J. Arid Environ. 105, 41–51. doi:10.1016/j.jaridenv.2014.02.015

U.S. BR-DO-MEB (Bureau of Reclamation Denver Office. Materials Engineering Branch), 1990. Earth Manual part 2, Third. ed. U.S. Government Printing Office, Denver, Colorado.

Van Genuchten, M., Leij, F., & Yates, S. (1991). *The RETC Code for Quantifying the Hydraulic Functions of Unsaturated Soils*. Retrieved from http://imel.mel.ar.wroc.pl/retc.pdf

Van Genuchten, M. T. (1980). A Closed-form Equation for Predicting the Hydraulic Conductivity of Unsaturated Soils, A - vg.pdf. *Soil Sci. Soc. Am. J*, *44*, 892–898. Retrieved from http://hydro.nevada.edu/courses/gey719/vg.pdf

Vrugt, J.A., van Wijk, M.T., Hopmans, J.W., Šimunek, J., 2001. One-, two-, and three-dimensional root water uptake functions for transient modeling. Water Resour. Res. 37, 2457–2470. doi:10.1029/2000WR000027

Whitley, D., 1994. A genetic algorithm tutorial. Stat. Comput. 4. doi:10.1007/BF00175354

Yao, T., Wierenga, P.J., Graham, A.R., Neuman, S.P., 2004. Neutron Probe Calibration in a Vertically Stratified Vadose Zone. Vadose Zo. J 1400–1406.